


# Flexible Capacitive Pressure Sensor Enhanced by Tilted Micropillar Arrays

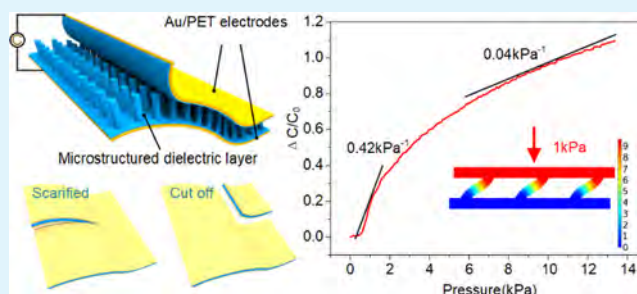
Yongsong Luo, Jinyou Shao,\* Shouren Chen, Xiaoliang Chen, Hongmiao Tian, Xiangming Li, Liang Wang, Duorui Wang, and Bingheng Lu

Micro- and Nano-Technology Research Center, State Key Laboratory for Manufacturing Systems Engineering, Xi'an Jiaotong University, Xi'an, Shaanxi 710049, China

## Supporting Information

**ABSTRACT:** Sensitivity of the sensor is of great importance in practical applications of wearable electronics or smart robotics. In the present study, a capacitive sensor enhanced by a tilted micropillar array-structured dielectric layer is developed. Because the tilted micropillars undergo bending deformation rather than compression deformation, the distance between the electrodes is easier to change, even discarding the contribution of the air gap at the interface of the structured dielectric layer and the electrode, thus resulting in high pressure sensitivity ( $0.42 \text{ kPa}^{-1}$ ) and very small detection limit (1 Pa). In addition, eliminating the presence of uncertain air gap, the dielectric layer is strongly bonded with the electrode, which makes the structure robust and endows the sensor with high stability and reliable capacitance response. These characteristics allow the device to remain in normal use without the need for repair or replacement despite mechanical damage. Moreover, the proposed sensor can be tailored to any size and shape, which is further demonstrated in wearable application. This work provides a new strategy for sensors that are required to be sensitive and reliable in actual applications.

**KEYWORDS:** capacitive, tilted micropillar array structures, flexible, pressure sensor, ultralight sensitivity



## ■ INTRODUCTION

Flexible pressure sensors have been attracting much attention due to their various potential applications, such as in human-machine interactive systems,<sup>1–3</sup> electronic skin,<sup>4–11</sup> health-care,<sup>12–19</sup> display touch screens,<sup>20–22</sup> and smart robotics.<sup>23–25</sup> Owing to the advantages of fast response times, low power consumption, good dynamic response, and temperature insensitivity, capacitive sensors with different materials or architectures have been widely researched. For example, capacitive sensors made using biocompatible flexible materials<sup>26,27</sup> or conductive fabric<sup>28–30</sup> can be integrated into a wearable textile to monitor human motions, such as breathing, speaking, and joint movement. Large-scale and flexible capacitive sensors with an ultrathin structure can be used as fully functional three-dimensional touch-pad devices, which can realize force and multitouch functions.<sup>31,32</sup>

In general, capacitive pressure sensors commonly possess a dielectric layer sandwiched between two electrodes. External pressures applied on capacitive sensors cause deformation of the dielectric layer, decreasing the distance between the two electrodes and thus leading to changes of the capacitance for external force measurement.<sup>33,34</sup> Making the dielectric layer more deformable is the key to improving the sensitivity of the sensors.<sup>15,26,35–37</sup> While using the highly compressible elastomeric materials with low Young's modulus, structuring the dielectric layer can effectively improve the sensitivity and

overcome the hysteresis caused by the viscoelastic behavior of materials. Zhang et al. utilized lotus leaf microstructures as the electrode template and microspheres as the dielectric layer to fabricate capacitive sensors with high sensitivity.<sup>38</sup> Guo et al. also utilized leaves and flowers as dielectric materials to fabricate highly sensitive capacitive sensors.<sup>39</sup> Bao's group developed a capacitive pressure sensor that employed micro-pyramid arrays as the dielectric layer. Pyramid cusps contacting with the electrode were easily deformed, leading to high sensitivity ( $0.55 \text{ kPa}^{-1}$ ).<sup>40</sup> Shim and co-workers reported a facile strategy for utilizing the air gap formed by the surface roughness of paper to develop a high-sensitivity capacitive pressure sensor ( $0.62 \text{ kPa}^{-1}$ ).<sup>32</sup> Although these approaches improve the sensitivity, the small contact area and the air gap existing at the interface of the microstructured dielectric layer and the counter electrode would result in the physical separation between the layers,<sup>29,31,41</sup> thus leading to poor structural robustness and stability. To avoid the above problems, it is necessary to integrate the electrodes and the dielectric layer into a stable and robust whole, which will inevitably remove the contribution of the air gap to the sensitivity,<sup>27,42,43</sup> thereby causing a contradiction between

**Received:** February 28, 2019

**Accepted:** April 22, 2019

**Published:** April 22, 2019

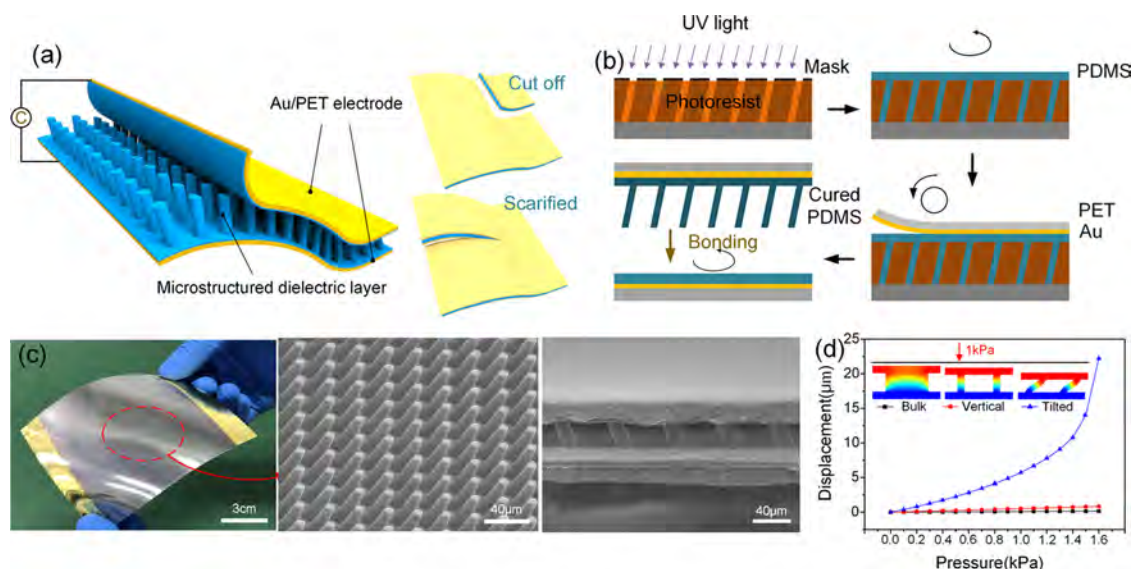


**Figure 1.** Schematic illustration of the capacitive pressure sensor. (a) The sensor architecture. Mechanical damages such as cuts or scratches do not affect the sensing performance. (b) Schematic diagram of the capacitive pressure sensor fabrication process. (c) Photographs and scanning electron microscopy (SEM) images showing the highly uniform micropillar array and flexible and ultrathin device. (d) Electrode displacement versus pressure curves of different structures, obtained by finite-element analysis (FEA).

sensitivity improvement and stability maintenance. Until now, simultaneously achieving high sensor sensitivity, stability, and reliability remains a major challenge.

In the present study, a flexible and ultrathin large-scale capacitive pressure sensor that satisfies the high-sensitivity, stability, and reliability requirements of various applications is presented. The proposed sensor is based on a poly-(dimethylsiloxane) (PDMS) dielectric layer structure with tilted micropillar arrays, which is highly uniform over a large area and strongly bonded to the Au-coated electrodes. Different from the traditional upright structure such as micropyramids, the tilted micropillar arrays exhibit bending deformation rather than compression deformation, making the distance between the two electrodes easier to decrease when force is applied. Owing to the resultant, the proposed sensor can exhibit a high sensitivity of  $0.42 \text{ kPa}^{-1}$ , much higher than that of the vertical structure ( $0.03 \text{ kPa}^{-1}$ ) and that of the bulk film ( $0.626 \text{ MPa}^{-1}$ ), even without the air-gap contribution, and it can be used for the detection of ultrasmall and light objects, such as grains and water drops. In addition, the dielectric layer is strongly bonded to the electrodes, eliminating the presence of uncertain air gaps and making the structure robust. There is no wear and slide at the interface and no change in the baseline capacitance before and after press, which endows the sensor with high stability and reliable capacitance response. Owing to the robust connection, the sensors remain highly consistent across multiple tests, with the relative standard deviation of less than 1.57%, and show no degradation in capacitance response after 1000 cycles. Moreover, the strong bonding allows the sensors to bear mechanical damages such as incidental scratches or cuts, without sudden failure or affecting the normal function, maintaining a continuous signal output. Precisely because of the uniform structure, these large-scale sensors can be cut into smaller pieces with the same sensing characteristics.

## RESULTS AND DISCUSSION

The proposed sensor comprises two flexible electrode plates and a dielectric layer with tilted micropillar arrays (Figure 1a). The dielectric layer is strongly bonded to the electrode by attaching the dielectric micropillar arrays closely onto the PDMS-coated counter electrode. The chemical bond formed after curing generates a strong connection between the electrode and the microstructures. A significant advantage of this sensor is that it can be cut into smaller sensors of arbitrary shape to satisfy different size and shape requirements. Each smaller sensor has the same sensing characteristics as those of the original large one, which means that individual sensors cut from the same sensor can replace each other. Meanwhile, even when suffering from mechanical damages, such as incidental scratches, cuts, or even cracks, the sensors still function normally without changes in the capacitance response to a constant pressure. During and after the process of damage, the sensors can provide continuous signal output without exhibiting sudden failure. Such advantages can be attributed to two main factors: (1) the proposed sensor contains highly uniform microstructures without air gaps at the interface of the microstructured PDMS layer and the electrode plate, resulting in each part of the sensor having the same reliable capacitance response under the same applied pressure; (2) the strong connection between the electrode and the microstructures enhances the stability of the device and can resist shear forces without sliding. Therefore, even when damaged, the proposed sensor can retain the original performance level, which is very important for its application in complex environments. For example, in robotic manipulator applications, even after being damaged by objects with sharp features, the sensors can maintain their original properties without repair, which means the signal could be output continuously without interruption, contrary to other reported traditional sensors<sup>44,45</sup> that lack this ability.

PDMS was selected as the dielectric material due to its good elastic properties and compatibility. The dielectric layer based on tilted micropillar arrays was fabricated by pouring and spin-

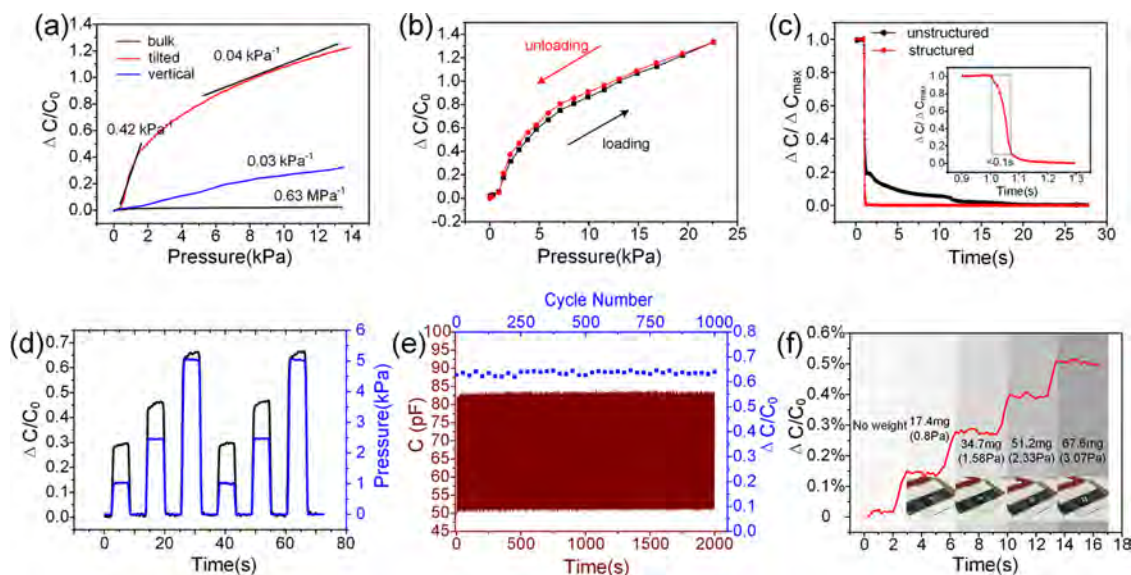


**Figure 2.** Typical pressure-sensing characteristics. (a) Pressure–response curves of the capacitive pressure sensors for dielectric layers with bulk film, vertical micropillar array, and tilted micropillar array. (b) Hysteresis characteristics of the pressure sensor. (c) Relaxation times of sensors with structured and unstructured dielectric layers. (d) Dynamic response of pressure sensors under periodic pressures of 1, 2.5, and 5 kPa. (e) Capacitance response of the pressure sensor during 1000 loading and unloading cycles. (f) Detection of ultralight-weight objects (grains of rice).

coating PDMS onto a tilted exposure photoresist mold. The tilt angle of the microstructure could be adjusted as a function of the exposure angle. Then, Au-coated poly(ethylene terephthalate) (PET) was applied on the template surface and then peeled off together with the PDMS layer after curing. The structured layer was finally placed on an uncured PDMS layer, with the top surface of the micropillars contacting the PDMS material (Figure 1b). Due to the curing procedure, the micropillars can be bonded to the residual PDMS layer on the counter electrode, forming a strong connection between the microstructured dielectric layer and the electrode plates. The strength of the connection can be up to 30 N (Figures S1 and S2, Supporting Information). This strategy can effectively achieve large-scale, flexible, and highly uniform microstructures over the entire substrate area, which can be seen from the highly parallel rows of tilted micropillars of identical height (Figure 1c). Such characteristics are very important for the large-area compatibility and uniformity of the capacitive pressure sensors, since the coplanar top surface of the micropillars determines a periodic and reproducible counter electrode plate, which means that any portion of the sensor has an indistinguishable functional structure. As it can be seen in Figure 1c, the fabricated device is ultrathin with a thickness of less than 100  $\mu\text{m}$ , whereas in the scanning electron microscopy (SEM) image, a remarkable contact without any air gaps at the interface of the electrode and the microstructures is demonstrated. Under external force application, the tilted micropillar arrays undergo bending deformation, which causes a larger change in the distance between the two electrodes compared to that caused by compression deformation.

Finite-element analysis (FEA) was used to investigate the deformation of different structures of same thickness (30  $\mu\text{m}$ ), including bulk film, vertical micropillar arrays, and tilted micropillar arrays with a tilt angle of 30° (Figure 1d). For the same applied pressure, the variation of the distance between the two electrodes with the tilted structures was much larger than that with the bulk film or the vertical structures. Under a pressure of 1 kPa, the top layer displacement of the tilted

structure was 10 and 70 times larger than that of the vertical structure and the bulk film, respectively, which means that the tilted microstructure strategy has a high potential for significantly improving the sensitivity.

The fabricated capacitive sensor was tested, and the effectiveness and feasibility of the proposed strategy were investigated from an experimental perspective. The measured pressure sensitivity of the three different structure types can be seen in Figure 2a. The pressure sensitivity  $S$  is defined as  $S = \delta(\Delta C/C_0)/\delta p$ , where  $p$  denotes the applied pressure and  $C$  and  $C_0$  the capacitances with and without the applied pressure, respectively. The bulk film sensor presented the lowest pressure sensitivity ( $0.626 \text{ MPa}^{-1}$ ), whereas the sensor with vertical microstructures showed an improved pressure sensitivity of  $0.033 \text{ kPa}^{-1}$  owing to its reduced dielectric layer stiffness. The sensor with tilted microstructures demonstrated the highest pressure sensitivity, which was  $0.42 \text{ kPa}^{-1}$  in the low-pressure regime ( $<1.5 \text{ kPa}$ ) and  $0.04 \text{ kPa}^{-1}$  in the high-pressure regime ( $>5 \text{ kPa}$ ). Such a high sensitivity can be attributed to two main factors: (1) large bending deformation can be generated with lower pressure compared to the compressive deformation generated in vertically microstructured sensors; and (2) air volume is replaced by PDMS when the structure is deformed, and PDMS has a higher dielectric constant ( $\sim 3$ ) than that of air (1).<sup>40,46</sup> Therefore, the capacitance increased due to the reduction in the distance between the two electrode plates according to factor (1) and was enhanced by the higher effective dielectric constant according to factor (2). In addition, the increase in sensitivity of the sensor with tilted micropillars in the  $<1.5 \text{ kPa}$  pressure range can be attributed to both the increase of the radial force component that generates bending deformation and the increase of the effective dielectric constant of the dielectric layer, since the air volume fraction decreases during bending deformation. The decrease in the slope of the red curve after 1.5 kPa was because the side of the micropillars came into contact with the bottom electrode and the bending deformation changed to compressive deformation (Figure S3,



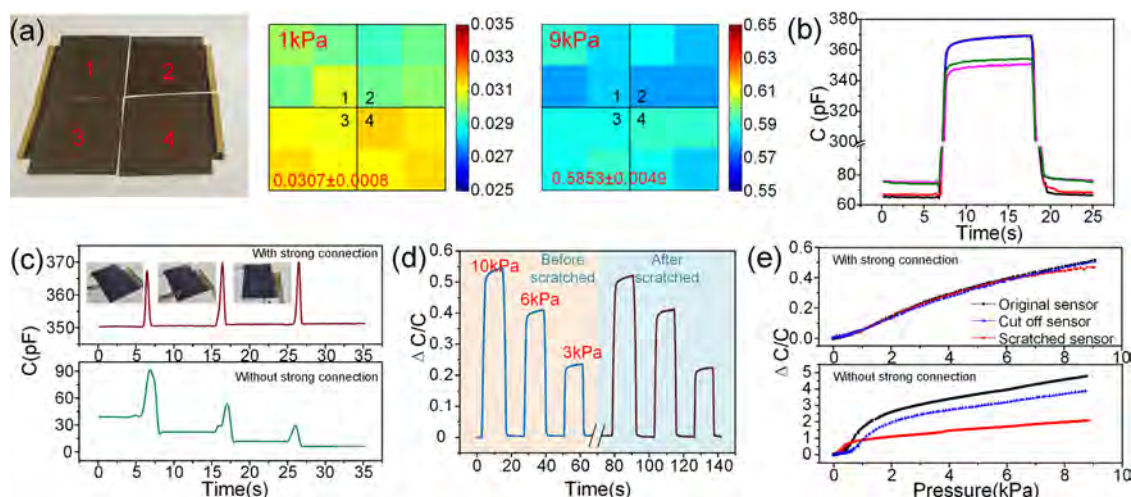


**Figure 3.** Pressure-sensing performance of scratched or cut sensors. (a) Image of the large sensor divided into four segments and mapping image of relative capacitance change distribution of the smaller sensor segments cut from the same sheet. Four areas defined by the intersection of the two center lines represented the four sensor segments, and the values corresponding to colors of four pixels inside each segment represented the relative capacitance change of each segment after testing four times. (b) Capacitance response curves of the same sensor that does not possess a strong connection between micropillars and electrodes under a pressure of 4 kPa for five independent tests without preload. The baseline values vary from 65 to 75 pF, and the response values vary from 352 to 369 pF. (c) Baseline capacitances of sensor segments with and without strong connection when suffering from three scratches, respectively, with insets showing the three scratches using a scalpel. For the segment with strong connection, the baseline capacitance increased rapidly from 350.4 to  $\sim 370$  pF and then returned to 350.6, 351.0, and 351.3 pF after the first, second, and third scratch, respectively. For the segment without strong connection, the baseline capacitance decreased from 39.1 to 22.2, 11.7, and 6.1 pF after three scratches. Both segments had an area of  $4 \times 4 \text{ cm}^2$ . (d) Capacitance response of a sensor segment to different pressures of 10, 6, and 3 kPa before (blue part of the curve) and after scratching (brown part of the curve). (e) Pressure–response curves of the original (black), the cut (blue), and the scratched sensor (red) of sensors with and without strong connection.

Supporting Information). The capacitance response of the capacitive sensor was affected by the tilting angle and the ratio of the micropillar diameter to the center-to-center distance (Figures S4 and S5, Supporting Information). Furthermore, the increase in the aspect ratio of the micropillars also causes an increase in the capacitance response. Considering the stability of the sensor, the structured dielectric layer must have sufficient strength to ensure that the initial shape of each pillar can be effectively maintained in the pressure-free state. When the number of micropillars per unit area is too small, it is difficult for the micropillars to return to the initial height under high pressure, which will cause inconsistency in the baseline capacitance. The sensor with  $30^\circ$  and ratio of 1:10 was chosen because it had a high capacitance response and the problem of instability was well solved.

In addition to improving the sensitivity, the micropillars also enhanced the relaxation property of the capacitive pressure sensor. The existence of voids in the microstructured film could contribute to storing and releasing of energy in a reversible manner during the elastic deformation of the microstructured surfaces, reducing the influence caused by the viscoelastic behavior of the PDMS dielectric layer.<sup>40</sup> Owing to this contribution, a reversible response with negligible hysteresis (Figure 2b) and decreased relaxation times (Figure 2c) could be achieved. The relaxation times of the pressure sensors with bulk film and tilted micropillar arrays were measured under cyclic loading and unloading of 8 kPa. A 90% constant was commonly used as the standard time value of the pressure sensors. The two types of sensors demonstrated significant differences in relaxation times, although only a slight difference in response times was observed (Figure S6, Supporting Information). The bulk film, due to the viscoelastic behavior of the PDMS film, demonstrated slow relaxation

times reaching up to 10 s, whereas the microstructured sensor exhibited a relaxation time of  $\sim 70$  ms shown in the inset, which was over 200 times shorter than that of the bulk film sensor. In fact, the response and the relaxation time depend on the testing platform, and the pressure could not be instantly applied. Therefore, the relaxation time would be shorter than  $\sim 70$  ms when ideal step pressure is applied. Due to the strong connection between the microstructure and the electrode plates, the sensor had constant baseline capacitance values during intermittent loading and unloading.

A reliable, continuous, stable, and perfectly repeatable sensing behavior was observed in the sensor with a remarkable match between the pressure input and the response curve under periodical pressures of 1, 2.5, and 5 kPa (Figure 2d). The strong connection also made the sensor demonstrate high mechanical strength, guaranteeing a long service life. To confirm the durability and stability of the sensor for long-term use, the capacitance response to an applied pressure of 4 kPa and 0.5 Hz for 1000 cycles was measured. The effective area of the sensor was about  $1.8 \times 2 \text{ cm}^2$ , and the baseline capacitance was about 50.6 pF, which was corresponding to  $14.1 \text{ pF cm}^{-2}$ . The capacitance of the sensor changed sharply from  $\sim 50$  to  $\sim 80$  pF under pressure loading and unloading. The baseline capacitance and the relative capacitance change showed little variation and no signal degradation during the 1000 cycles (Figure 2e). The sensor also showed good durability after hundreds of bending cycles (Figure S7, Supporting Information). To verify its detection limit and resolution, four grains of rice were placed on the sensor one by one. As it can be seen in Figure 2f, the capacitance response demonstrated a “stepped” escalation every time a grain of rice was placed on the sensor. The inset shows the progress from putting one grain to five grains of rice and corresponds to each step of the curve. The

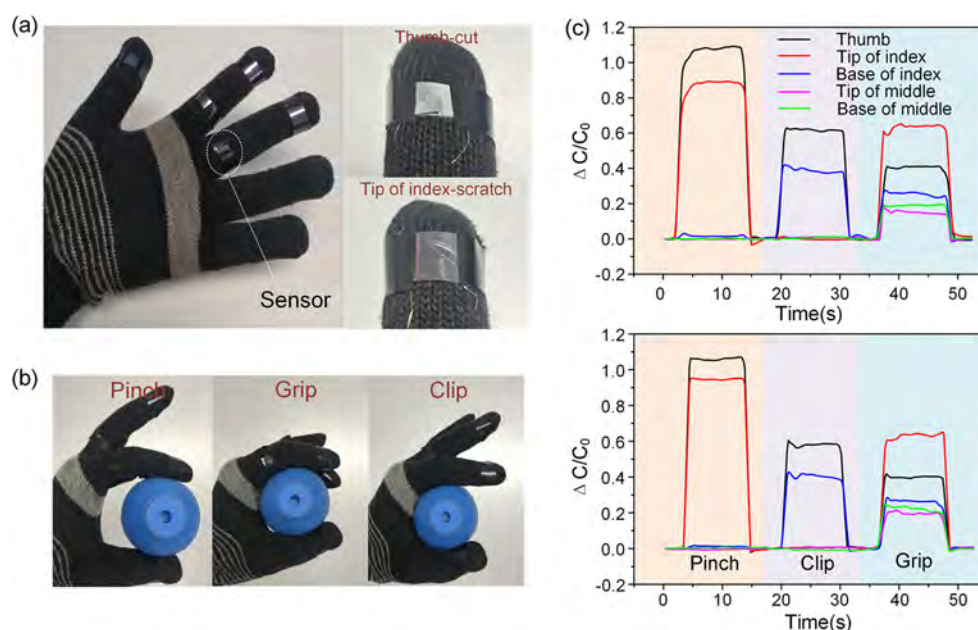


**Figure 4.** (a) Glove integrated with five sensors cut from the same sensor sheet, and images of the sensors on the thumb and the top of the index suffered damaged by cut and scratch, respectively. (b) Hand postures used to grasp objects categorized as pinching, clipping, and gripping. (c) Capacitance response curves of the five sensors before (top) and after (bottom) mechanical damage. The top and bottom graphs correspond to the capacitance responses of all five sensors on the different fingers before and after damage, respectively, and the three sections of each graph correspond to the hand postures of pinching, clipping, and gripping.

average grain weight was  $\sim 17$  mg, which corresponded to a very small pressure of only 1 Pa. In practice, the detection limit is a very important parameter for measuring ultrasmall forces such as air, sound waves, and small mechanical vibrations. In addition, the high resolution of the sensor was depicted by the clearly discernible steps on the response curve every time the number of grains was changed.

In practical applications, sensors of different shapes and sizes are required depending on the requirements. However, it is very costly to design and manufacture individual sensors with specific size and shape for specific demands. Owing to the highly uniform microstructure and the absence of air gaps, the proposed sensors can be cut into smaller pieces of different sizes and shapes with identical sensing characteristics. The consistency and repeatability of cut sensor pieces were verified through experiments. A large-area sensor ( $8 \times 8$  cm<sup>2</sup>) was fabricated using the above-described method and then cut into four pieces to investigate the sensing response of each sensor to different pressures. In Figure 3a, the mapping image of the  $\Delta C/C_0$  distribution is presented, displaying the consistency of sensors cut from the large one, showing also the repeatability of each sensor segment. The four sensor segments revealed a highly uniform distribution of  $\Delta C/C_0$  with a small standard deviation of 0.0008 at 1 kPa and 0.0049 at 9 kPa, corresponding to a relative standard deviation of 2.60% at 1 kPa and 0.84% at 9 kPa. The results of a single segment demonstrated that the relative standard deviation for repeated measurements was  $<1.57\%$  at 1 kPa and  $<0.80\%$  at 9 kPa, whereas the sensor without a strong bonding demonstrated inconsistent and unreliable response (Figure 3b).

In addition, in real-life applications, the mechanical compliance and stability of the pressure sensors are as important and necessary as sensitivity. Sensors are usually subjected to mechanical damages, such as incidental scratches or cuts, which affect the sensing performance or even lead to

failure. The usual solution to damage is replacement or repair of the device. However, replacement or repair will interrupt the signal output, making the time-domain signal discontinuous, which is a serious problem in real-time monitoring. Due to the strong connection between micropillar arrays and electrodes, the proposed capacitive pressure sensors can bear mechanical damages and maintain the continuous signal output without sudden failure. One sensor segment ( $4 \times 4$  cm<sup>2</sup>) was scratched three times using a scalpel (Figure 3c). For the sensor with a strong connection between the dielectric layer and electrodes, these minor changes in the baseline capacitance value after three scratches indicated that no sliding occurred between the two electrodes due to the strong bonding. If the microstructured dielectric layer is physically separated from the electrode plate without a strong connection, the contact area between the microstructured layer and the electrode plate becomes unstable and the air gap will change during scratching, thus resulting in a significant change in baseline capacitance. The capacitance response of a second sensor segment was measured at different pressures of 10, 6, and 3 kPa, as shown in Figure 3d. In the next step, the same sensor segment was scratched. The capacitance response of the scratched sensor under the same pressures was actually similar to that of the sensor before scratching. Other reported sensors with random or aperiodic structures cannot provide unchanged sensing characteristics when cut into pieces because each portion of the structure has a unique architecture. Figure 3e shows the relative capacitance change versus pressure change. For the sensors with a strong connection, the three curves demonstrated a remarkable degree of overlap, showing that the three sensors have almost the same sensing characteristics. This further indicates that damage has little influence on the sensor, whether it is scratched or cut into pieces, whereas the physically separated sensor without strong connection will be seriously affected by the mechanical damage as the other three

curves show. The curve of the scratched sensor with a strong connection is slightly offset from the other two in the range above 7 kPa, which was probably a result of plastic deformation at the edge of the scratch. The deformation on both sides of the scratch would overlap partially to induce pressure to focus on the overlap, thus reducing the actual pressure on the whole surface, leading to a decrease in the relative capacitance change. The relative capacitance change of the scratched sensor rose up to the value of the intact sensor, since no overlap occurred along the scratch.

Due to the advantage of being able to function without any change in capacitance response when damaged, the proposed sensor has the potential to be used in harsh environments, where a sensor may be scratched or cut. To investigate the applicability of the proposed sensor, several sensors were integrated onto a glove to recognize the hand posture and track the pressures on each finger when picking up an object (Figure 4). Each sensor on the glove was cut off from the same sensor so as to ensure same sensing characteristics. The sensors were attached to the thumb, the top of the index, the base of the index, and the top and the base of the middle finger. Micro-coaxial cables embedded in the glove were employed to minimize the mutual capacitance caused by wiring. Change in the capacitance caused by external conductors such as human body was negligible compared with that caused by touching force (Figure S8, Supporting Information).

In application, the glove was used to grasp some objects with sharp features such as blades, tool bits, and even a cactus plant. During these processes, sensors frequently touching the sharp parts of these objects would be scratched or even sliced. It can be seen that the surface of the sensors attached to the thumb and the top of the index were heavily worn or even torn (Figure 4a). The responses of the sensors when wearing the glove to grab an object were compared before and after damages. The hand postures tested in this study were categorized as pinching (by using thumb and the top of another finger), clipping (by using thumb and the base of another finger), and gripping (by using all of the fingers) (Figure 4b). The electrical signal of the sensors during pinching, clipping, and gripping a ball were recorded. It was demonstrated that although the sensors were damaged to varying degrees, they could still achieve almost the same capacitance response as that prior to damage (Figure 4c). The capacitance values vary with different ways of grasping the object, which provided the basis for distinguishing different postures by comparing the capacitance change of each sensor to that of the others. For example, in the first section of the graph, the sharp increase in capacitance of sensors attached to the thumb and the top of the index indicated that the object was pinched by the thumb and the top of the index. Besides, all of the sensors used in this experiment were cut from the same sheet, having the same sensing characteristics, and therefore the pressure magnitude on each finger could be inferred by comparing the relative capacitance change of the sensors. Moreover, it can be deduced from the first section of the graphs that the pressure on the thumb is higher than the pressure on the top of the index when pinching the object. Sensors used in harsh environments would usually face the possibility of being damaged, which would require their replacement so as not to interfere with the normal function. However, the proposed sensors integrated on the glove were able to function adequately even with severe scratches and thus there is no need to interrupt a process for the replacement of a

damaged sensor. The response curves exhibit the same trend, from which the different postures can be distinguished and pressure magnitudes on different fingers can be determined.

## CONCLUSIONS

In summary, a new capacitive pressure sensor, based on a structured dielectric layer with tilted micropillar arrays, with high sensitivity, stability, and reliability was demonstrated. The dielectric layer was strongly bonded with the electrode plates, eliminating the influence of air gaps that may lead to uncertain capacitance values. The bending deformation of the tilted micropillar arrays replaced the compression deformation of the traditional vertical structures, facilitating the changes in distance between the two electrodes even under very small pressure levels, which resulted in a remarkable increase in sensitivity. The proposed sensor demonstrated a sensitivity of  $0.42 \text{ kPa}^{-1}$  in the low-pressure regime and  $0.04 \text{ kPa}^{-1}$  in the high-pressure regime, which was significantly higher than that of the bulk film sensor but was in the same order of magnitude with that of the sensors that use air gaps or a small contact area for increasing sensitivity. Moreover, the proposed sensor was able to detect the weight of one grain of rice, which corresponded to a pressure of 1 Pa. The viscoelastic properties of PDMS were efficiently reduced by the micropillar arrays so that the sensor exhibited negligible hysteresis and short relaxation times. In addition, the strong bonding between the dielectric layer and the electrodes not only eliminated the uncertainty of the capacitance response induced by the air gap but also strengthened the structure of the sensor. Under repeated loading and unloading cycles, the sensor produced repeatable and reproducible signals, whereas the capacitance response showed no decay over 1000 cycles. Moreover, the sensor function was not affected by damages, such as scratches or cuts. Besides, sensor segments cut from the same sensor displayed similar sensing characteristics. Based on this characteristic, sensors cut off from the same sensor sheet were integrated onto a glove, and hand postures were able to be distinguished, whereas the pressure magnitudes on each finger could be identified by the capacitance response of each sensor, even when suffering from mechanical damages.

## EXPERIMENTAL SECTION

**Preparation of Photoresist Template.** The photoresist (AZ P4620) was spin-coated on a silicon wafer at 1000 rpm for 30 s and then soft-baked at  $95^\circ\text{C}$  for 5 min. The procedure was repeated twice to obtain films  $\sim 30 \text{ }\mu\text{m}$  thick. A photomask containing a pattern of microhole arrays ( $10 \text{ }\mu\text{m}$  in diameter) was pressed with the patterned surface contacting against the photoresist. The assembly was placed on the stage of goniometers and then obliquely exposed to UV light for 90 s by adjusting the angle between the stage and the horizontal plane to  $30^\circ$  to obtain the template after the development process.

**Fabrication of Sensor.** PDMS (Sylgard 184, Dow Corning) with 10:1 mass ratio of base to cross-linker was poured onto the photoresist on the template. Then, the assembly was placed into a vacuum chamber for  $\sim 5 \text{ min}$  to remove air from the cavities. In the next step, the PDMS was spin-coated on the template at 8000 rpm for 50 s to ensure an ultrathin residual layer of  $\sim 5 \text{ }\mu\text{m}$ . Next, the poly(ethylene terephthalate) (PET) foil deposited with Cr, Au, and  $\text{SiO}_2$  was applied on the template surface with the  $\text{SiO}_2$  layer facing the PDMS layer. The Au layer (100 nm) was the electrode, and the Cr layer (20 nm) was used to enhance the cohesiveness between Au and PET and between Au and  $\text{SiO}_2$ .  $\text{SiO}_2$  was used as the medium to bond PDMS onto the PET substrate. Subsequently, the duplicated PDMS was cured at  $50^\circ\text{C}$  for 8 h and then peeled off from the template with the PET foil. The structured PDMS was finally placed



on an uncured PDMS layer, which was also spin-coated at 8000 rpm for 50 s on the PET foil and then cured at 80 °C for 1 h to form the capacitor.

**Characterization.** The structural morphologies were examined by scanning electron microscopy (SU8010, HITACHI). A thin layer of gold (~10 nm) was coated on the PDMS layer before imaging with SEM, and the accelerating voltage was 5 kV. Capacitance measurements were performed at 100 kHz using a semiconductor analyzer (B1500A, Agilent). A highly configurable single-column testing machine (ESM303, Mark-10) was used to apply dynamic pressures. Sensors were placed on the horizontal platform of the testing machine. Elastic compression fixtures with different sizes were employed to press the sensor for uniform deformation. The frequency and dimension of the load can be controlled by adjusting the speed and displacement. A force gauge (M5-10, Mark-10) was employed to record the force.

## ■ ASSOCIATED CONTENT

### ■ Supporting Information

The Supporting Information is available free of charge on the ACS Publications website at DOI: 10.1021/acsami.9b03718.

SEM images of the strong connections between micropillars and electrodes; connection strength test between the microstructures and the electrodes; optical images of the deformation process of the micropillars under pressure; influence of the tilting angle of the micropillars on capacitance response and the baseline capacitance per unit area; influence of the ratio of the micropillar diameter to the distance of center of the circle on capacitance response; response times of sensors with an unstructured dielectric layer and a structured dielectric layer; bending durability test of the sensor; and capacitance response from the proximity of human finger to the touch (PDF)

## ■ AUTHOR INFORMATION

### Corresponding Author

\*E-mail: jyshao@mail.xjtu.edu.cn.

### ORCID

Jinyou Shao: 0000-0003-2525-4587

### Notes

The authors declare no competing financial interest.

## ■ ACKNOWLEDGMENTS

Research was supported by the Major Research Plan of NSFC on Nanomanufacturing (Grant Number 91323303), NSFC Funds (Grant Number 51522508), and the Natural Science Foundation of Shaanxi Province of China (2016JM5086).

## ■ REFERENCES

- (1) Takamatsu, S.; Lonjaret, T.; Ismailova, E.; Masuda, A.; Itoh, T.; Malliaras, G. G. Wearable Keyboard Using Conducting Polymer Electrodes on Textiles. *Adv. Mater.* **2016**, *28*, 4485–4488.
- (2) Kim, K. K.; Hong, S.; Cho, H. M.; Lee, J.; Suh, Y. D.; Ham, J.; Ko, S. H. Highly Sensitive and Stretchable Multidimensional Strain Sensor with Prestrained Anisotropic Metal Nanowire Percolation Networks. *Nano Lett.* **2015**, *15*, 5240–5247.
- (3) Wang, C.; Hwang, D.; Yu, Z.; Takei, K.; Park, J.; Chen, T.; Ma, B.; Javey, A. User-Interactive Electronic Skin for Instantaneous Pressure Visualization. *Nat. Mater.* **2013**, *12*, 899–904.
- (4) Amjadi, M.; Kyung, K.-U.; Park, I.; Sitti, M. Stretchable, Skin-Mountable, and Wearable Strain Sensors and Their Potential Applications: A Review. *Adv. Funct. Mater.* **2016**, *26*, 1678–1698.

- (5) Wang, C.; Li, X.; Gao, E.; Jian, M.; Xia, K.; Wang, Q.; Xu, Z.; Ren, T.; Zhang, Y. Carbonized Silk Fabric for Ultrastretchable, Highly Sensitive, and Wearable Strain Sensors. *Adv. Mater.* **2016**, *28*, 6640–6648.
- (6) Pang, Y.; Zhang, K.; Yang, Z.; Jiang, S.; Ju, Z.; Li, Y.; Wang, X.; Wang, D.; Jian, M.; Zhang, Y.; Liang, R.; Tian, H.; Yang, Y.; Ren, T. L. Epidermis Microstructure Inspired Graphene Pressure Sensor with Random Distributed Spinosum for High Sensitivity and Large Linearity. *ACS Nano* **2018**, *12*, 2346–2354.
- (7) Hua, Q.; Sun, J.; Liu, H.; Bao, R.; Yu, R.; Zhai, J.; Pan, C.; Wang, Z. L. Skin-Inspired Highly Stretchable and Conformable Matrix Networks for Multifunctional Sensing. *Nat. Commun.* **2018**, *9*, No. 244.
- (8) Takei, K.; Takahashi, T.; Ho, J. C.; Ko, H.; Gillies, A. G.; Leu, P. W.; Fearing, R. S.; Javey, A. Nanowire Active-Matrix Circuitry for Low-Voltage Macroscale Artificial Skin. *Nat. Mater.* **2010**, *9*, 821–826.
- (9) Yamada, T.; Hayamizu, Y.; Yamamoto, Y.; Yomogida, Y.; Izadi-Najafabadi, A.; Futaba, D. N.; Hata, K. A Stretchable Carbon Nanotube Strain Sensor for Human-Motion Detection. *Nat. Nanotechnol.* **2011**, *6*, 296–301.
- (10) Kim, K. H.; Jang, N. S.; Ha, S. H.; Cho, J. H.; Kim, J. M. Highly Sensitive and Stretchable Resistive Strain Sensors Based on Microstructured Metal Nanowire/Elastomer Composite Films. *Small* **2018**, *14*, No. 1704232.
- (11) Nie, B.; Li, X.; Shao, J.; Li, X.; Tian, H.; Wang, D.; Zhang, Q.; Lu, B. Flexible and Transparent Strain Sensors with Embedded Multiwalled Carbon Nanotubes Meshes. *ACS Appl. Mater. Interfaces* **2017**, *9*, 40681–40689.
- (12) Choi, S.; Lee, H.; Ghaffari, R.; Hyeon, T.; Kim, D. H. Recent Advances in Flexible and Stretchable Bio-Electronic Devices Integrated with Nanomaterials. *Adv. Mater.* **2016**, *28*, 4203–4218.
- (13) Khan, Y.; Ostfeld, A. E.; Lochner, C. M.; Pierre, A.; Arias, A. C. Monitoring of Vital Signs with Flexible and Wearable Medical Devices. *Adv. Mater.* **2016**, *28*, 4373–4395.
- (14) Trung, T. Q.; Lee, N. E. Flexible and Stretchable Physical Sensor Integrated Platforms for Wearable Human-Activity Monitoring and Personal Healthcare. *Adv. Mater.* **2016**, *28*, 4338–4372.
- (15) Pang, C.; Koo, J. H.; Nguyen, A.; Caves, J. M.; Kim, M. G.; Chortos, A.; Kim, K.; Wang, P. J.; Tok, J. B.; Bao, Z. Highly Skin-Conformal Microhair Sensor for Pulse Signal Amplification. *Adv. Mater.* **2015**, *27*, 634–640.
- (16) Chen, X.; Shao, J.; An, N.; Li, X.; Tian, H.; Xu, C.; Ding, Y. Self-Powered Flexible Pressure Sensors with Vertically Well-Aligned Piezoelectric Nanowire Arrays for Monitoring Vital Signs. *J. Mater. Chem. C* **2015**, *3*, 11806–11814.
- (17) Schwartz, G.; Tee, B. C.; Mei, J.; Appleton, A. L.; Kim, D. H.; Wang, H.; Bao, Z. Flexible Polymer Transistors with High Pressure Sensitivity for Application in Electronic Skin and Health Monitoring. *Nat. Commun.* **2013**, *4*, No. 1859.
- (18) Kang, D.; Pikhitsa, P. V.; Choi, Y. W.; Lee, C.; Shin, S. S.; Piao, L.; Park, B.; Suh, K. Y.; Kim, T. I.; Choi, M. Ultrasensitive Mechanical Crack-Based Sensor Inspired by the Spider Sensory System. *Nature* **2014**, *516*, 222–226.
- (19) Chen, X.; Li, X.; Shao, J.; An, N.; Tian, H.; Wang, C.; Han, T.; Wang, L.; Lu, B. High-Performance Piezoelectric Nanogenerators with Imprinted P(VDF-TrFE)/BaTiO<sub>3</sub> Nanocomposite Micropillars for Self-Powered Flexible Sensors. *Small* **2017**, *13*, No. 1604245.
- (20) Cho, S.; Kang, S.; Pandya, A.; Shanker, R.; Khan, Z.; Lee, Y.; Park, J.; Craig, S. L.; Ko, H. Large-Area Cross-Aligned Silver Nanowire Electrodes for Flexible, Transparent, and Force-Sensitive Mechanochromic Touch Screens. *ACS Nano* **2017**, *11*, 4346–4357.
- (21) Kim, C. C.; Lee, H. H.; Oh, K. H.; Sun, J. Y. Highly Stretchable, Transparent Ionic Touch Panel. *Science* **2016**, *353*, 682–687.
- (22) Paeng, D.; Yoo, J. H.; Yeo, J.; Lee, D.; Kim, E.; Ko, S. H.; Grigoropoulos, C. P. Low-Cost Facile Fabrication of Flexible Transparent Copper Electrodes by Nanosecond Laser Ablation. *Adv. Mater.* **2015**, *27*, 2762–2767.

- (23) Shi, G.; Zhao, Z.; Pai, J.-H.; Lee, I.; Zhang, L.; Stevenson, C.; Ishara, K.; Zhang, R.; Zhu, H.; Ma, J. Highly Sensitive, Wearable, Durable Strain Sensors and Stretchable Conductors Using Graphene/Silicon Rubber Composites. *Adv. Funct. Mater.* **2016**, *26*, 7614–7625.
- (24) Gong, S.; Lai, D. T.; Wang, Y.; Yap, L. W.; Si, K. J.; Shi, Q.; Jason, N. N.; Sridhar, T.; Uddin, H.; Cheng, W. Tattoo-like Polyaniline Microparticle-Doped Gold Nanowire Patches as Highly Durable Wearable Sensors. *ACS Appl. Mater. Interfaces* **2015**, *7*, 19700–19708.
- (25) Kim, J.; Lee, M.; Shim, H. J.; Ghaffari, R.; Cho, H. R.; Son, D.; Jung, Y. H.; Soh, M.; Choi, C.; Jung, S.; Chu, K.; Jeon, D.; Lee, S. T.; Kim, J. H.; Choi, S. H.; Hyeon, T.; Kim, D. H. Stretchable Silicon Nanoribbon Electronics for Skin Prosthesis. *Nat. Commun.* **2014**, *5*, No. 5747.
- (26) Boutry, C. M.; Nguyen, A.; Lawal, Q. O.; Chortos, A.; Rondeau-Gagne, S.; Bao, Z. A Sensitive and Biodegradable Pressure Sensor Array for Cardiovascular Monitoring. *Adv. Mater.* **2015**, *27*, 6954–6961.
- (27) Gerratt, A. P.; Michaud, H. O.; Lacour, S. P. Elastomeric Electronic Skin for Prosthetic Tactile Sensation. *Adv. Funct. Mater.* **2015**, *25*, 2287–2295.
- (28) Viry, L.; Levi, A.; Totaro, M.; Mondini, A.; Mattoli, V.; Mazzolai, B.; Beccai, L. Flexible Three-Axial Force Sensor for Soft and Highly Sensitive Artificial Touch. *Adv. Mater.* **2014**, *26*, 2659–2664.
- (29) Atalay, O.; Atalay, A.; Gafford, J.; Walsh, C. A Highly Sensitive Capacitive-Based Soft Pressure Sensor Based on a Conductive Fabric and a Microporous Dielectric Layer. *Adv. Mater. Technol.* **2018**, *3*, No. 1700237.
- (30) Atalay, A.; Sanchez, V.; Atalay, O.; Vogt, D. M.; Haufe, F.; Wood, R. J.; Walsh, C. J. Batch Fabrication of Customizable Silicone-Textile Composite Capacitive Strain Sensors for Human Motion Tracking. *Adv. Mater. Technol.* **2017**, *2*, No. 1700136.
- (31) Kim, H.; Kim, G.; Kim, T.; Lee, S.; Kang, D.; Hwang, M. S.; Chae, Y.; Kang, S.; Lee, H.; Park, H. G.; Shim, W. Transparent, Flexible, Conformal Capacitive Pressure Sensors with Nanoparticles. *Small* **2018**, *14*, No. 1870032.
- (32) Lee, K.; Lee, J.; Kim, G.; Kim, Y.; Kang, S.; Cho, S.; Kim, S.; Kim, J. K.; Lee, W.; Kim, D. E.; Kang, S.; Kim, D.; Lee, T.; Shim, W. Rough-Surface-Enabled Capacitive Pressure Sensors with 3D Touch Capability. *Small* **2017**, *13*, No. 1700368.
- (33) Yao, S.; Zhu, Y. Wearable Multifunctional Sensors Using Printed Stretchable Conductors Made of Silver Nanowires. *Nanoscale* **2014**, *6*, 2345–2352.
- (34) Lipomi, D. J.; Vosgueritchian, M.; Tee, B. C.; Hellstrom, S. L.; Lee, J. A.; Fox, C. H.; Bao, Z. Skin-Like Pressure and Strain Sensors Based on Transparent Elastic Films of Carbon Nanotubes. *Nanotechnol.* **2011**, *6*, 788–792.
- (35) Park, S.; Kim, H.; Vosgueritchian, M.; Cheon, S.; Kim, H.; Koo, J. H.; Kim, T. R.; Lee, S.; Schwartz, G.; Chang, H.; Bao, Z. Stretchable Energy-Harvesting Tactile Electronic Skin Capable of Differentiating Multiple Mechanical Stimuli Modes. *Adv. Mater.* **2014**, *26*, 7324–7332.
- (36) Tee, B. C. K.; Chortos, A.; Dunn, R. R.; Schwartz, G.; Eason, E.; Bao, Z. Tunable Flexible Pressure Sensors Using Microstructured Elastomer Geometries for Intuitive Electronics. *Adv. Funct. Mater.* **2014**, *24*, 5427–5434.
- (37) Shao, J.; Chen, X.; Li, X.; Tian, H.; Wang, C.; Lu, B. Nanoimprint Lithography for the Manufacturing of Flexible Electronics. *Sci. China: Technol. Sci.* **2019**, *62*, 175–198.
- (38) Li, T.; Luo, H.; Qin, L.; Wang, X.; Xiong, Z.; Ding, H.; Gu, Y.; Liu, Z.; Zhang, T. Flexible Capacitive Tactile Sensor Based on Micropatterned Dielectric Layer. *Small* **2016**, *12*, 5042–5048.
- (39) Wan, Y.; Qiu, Z.; Huang, J.; Yang, J.; Wang, Q.; Lu, P.; Yang, J.; Zhang, J.; Huang, S.; Wu, Z.; Guo, C. F. Natural Plant Materials as Dielectric Layer for Highly Sensitive Flexible Electronic Skin. *Small* **2018**, *14*, No. 1801657.
- (40) Mannsfeld, S. C.; Tee, B. C.; Stoltenberg, R. M.; Chen, C. V.; Barman, S.; Muir, B. V.; Sokolov, A. N.; Reese, C.; Bao, Z. Highly Sensitive Flexible Pressure Sensors with Microstructured Rubber Dielectric Layers. *Nat. Mater.* **2010**, *9*, 859–864.
- (41) Joo, Y.; Yoon, J.; Ha, J.; Kim, T.; Lee, S.; Lee, B.; Pang, C.; Hong, Y. Highly Sensitive and Bendable Capacitive Pressure Sensor and Its Application to 1 V Operation Pressure-Sensitive Transistor. *Adv. Electron. Mater.* **2017**, *3*, No. 1600455.
- (42) Chen, S.; Zhuo, B.; Guo, X. Large Area One-Step Facile Processing of Microstructured Elastomeric Dielectric Film for High Sensitivity and Durable Sensing over Wide Pressure Range. *ACS Appl. Mater. Interfaces* **2016**, *8*, 20364–20370.
- (43) Pyo, S.; Choi, J.; Kim, J. Flexible, Transparent, Sensitive, and Crosstalk-Free Capacitive Tactile Sensor Array Based on Graphene Electrodes and Air Dielectric. *Adv. Electron. Mater.* **2018**, *4*, No. 1700427.
- (44) He, Y.; Liao, S.; Jia, H.; Cao, Y.; Wang, Z.; Wang, Y. A Self-Healing Electronic Sensor Based on Thermal-Sensitive Fluids. *Adv. Mater.* **2015**, *27*, 4622–4627.
- (45) Tee, B. C.; Wang, C.; Allen, R.; Bao, Z. An Electrically and Mechanically Self-Healing Composite with Pressure- and Flexion-Sensitive Properties for Electronic Skin Applications. *Nat. Nanotechnol.* **2012**, *7*, 825–832.
- (46) Kwon, D.; Lee, T. I.; Shim, J.; Ryu, S.; Kim, M. S.; Kim, S.; Kim, T. S.; Park, I. Highly Sensitive, Flexible, and Wearable Pressure Sensor Based on a Giant Piezocapacitive Effect of Three-Dimensional Microporous Elastomeric Dielectric Layer. *ACS Appl. Mater. Interfaces* **2016**, *8*, 16922–16931.